Eigenvalue Spectra of Modular Networks

Tiago P. Peixoto*

Institut für Theoretische Physik, Universität Bremen, Hochschulring 18, D-28359 Bremen, Germany

(Received 11 June 2013; published 26 August 2013)

A large variety of dynamical processes that take place on networks can be expressed in terms of the spectral properties of some linear operator which reflects how the dynamical rules depend on the network topology. Often, such spectral features are theoretically obtained by considering only local node properties, such as degree distributions. Many networks, however, possess large-scale modular structures that can drastically influence their spectral characteristics and which are neglected in such simplified descriptions. Here, we obtain in a unified fashion the spectrum of a large family of operators, including the adjacency, Laplacian, and normalized Laplacian matrices, for networks with generic modular structure, in the limit of large degrees. We focus on the conditions necessary for the merging of the isolated eigenvalues with the continuous band of the spectrum, after which the planted modular structure can no longer be easily detected by spectral methods. This is a crucial transition point which determines when a modular structure is strong enough to affect a given dynamical process. We show that this transition happens in general at different points for the different matrices, and hence the detectability threshold can vary significantly, depending on the operator chosen. Equivalently, the sensitivity to the modular structure of the different dynamical processes associated with each matrix will be different, given the same large-scale structure present in the network. Furthermore, we show that, with the exception of the Laplacian matrix, the different transitions coalesce into the same point for the special case where the modules are homogeneous but separate otherwise.

DOI: 10.1103/PhysRevLett.111.098701 PACS numbers: 89.75.Hc, 02.70.Hm, 05.10.−a, 64.60.aq

Networks form the substrate of a dominating class of interacting complex systems, on which various dynamical processes take place. Many of the most important types of dynamics, such as random walks [1,2], diffusion, synchronization [3–5], and epidemic spreading [6–8], have central properties which are directly expressed via the spectral features of matrices associated with the network topology [9–11], such as the mixing time of random walks, epidemic thresholds, and the synchronization speed of oscillators, to name a few. Virtually all of these processes will be affected by large-scale modular structures present in the network [12], which is reflected in its spectral properties [13–16]. Since such large-scale modularity is a ubiquitous property in real networks [12], describing the spectral features resulting from this is a crucial step in understanding how these systems function. Additionally, the information encoded in the eigenvectors of these matrices are central to the nontrivial task of detecting large-scale features in empirical networks [16–20], and from it, it is possible to derive general bounds on the detectability of existing community structure [16].

In this work, we formulate a unified framework to obtain the eigenvalue spectrum associated with arbitrary modular structures, parametrized as stochastic block models [21–24]. The framework allows the straightforward calculation of a large class of matrices which include the adjacency, Laplacian, and normalized Laplacian matrices, and is exact in the limit of large degrees. It contrasts with previous work [14], which is exact in the limit of small degrees, but depends on the solution of a number of self-consistency equations which are solved stochastically. Here, we show that if the block structure is sufficiently well pronounced, it will trigger the appearance of isolated eigenvalues, with associated eigenvectors strongly correlated with the block partition. If the block structure becomes too weak (but nonvanishing), the isolated eigenvalues merge with the continuous band, and the eigenvectors are no longer correlated with the block partition. This has important consequences to the detectability of modular structure in networks [16] but also to a large class of dynamical processes, since after this transition takes place, one should not expect the modular structure to play a significant role. We show that in general the different matrices have different sensitivities to the imposed block structure and exhibit these transitions for different modularity strengths.

Unified framework.—Any given undirected network can be encoded via its adjacency matrix $\boldsymbol{A}$, which has entries $A_{ij} = 1$ if node i is adjacent to i, or $A_{ij} = 0$ otherwise. The Laplacian matrix is defined as $\boldsymbol{L} = \boldsymbol{D} - \boldsymbol{A}$, where $\boldsymbol{D}$ is a diagonal matrix containing the vertex degrees $D_{ij} = \delta_{ij}k_i$. Finally, the normalized Laplacian is defined as $\boldsymbol{\mathcal{L}} = \boldsymbol{I} - \boldsymbol{D}^{-1/2}\boldsymbol{A}\boldsymbol{D}^{-1/2}$. Here, we use a general parametrization which contains these matrices as special cases, via the matrix $\boldsymbol{W} = \boldsymbol{C} + \boldsymbol{M}$, where $\boldsymbol{C}$ is a random diagonal matrix, and $\boldsymbol{M}$ is a random symmetric matrix. Simply by choosing $\{\boldsymbol{C} = 0, \boldsymbol{M} = \boldsymbol{A}\}$, $\{\boldsymbol{C} = D, \boldsymbol{M} = -\boldsymbol{A}\}$, and $\{\boldsymbol{C} = \boldsymbol{I}, \boldsymbol{M} = -\boldsymbol{D}^{-1/2}\boldsymbol{A}\boldsymbol{D}^{-1/2}\}$, we recover $\boldsymbol{A}$, $\boldsymbol{L}$, and $\boldsymbol{\mathcal{L}}$, respectively. We may write $\boldsymbol{W} = \boldsymbol{C} + \boldsymbol{\mathcal{M}} + \langle \boldsymbol{M} \rangle = \boldsymbol{\mathcal{X}} + \langle \boldsymbol{M} \rangle$, such that

the matrix $\mathcal{X} = \boldsymbol{C} + \mathcal{M}$, with $\mathcal{M} = \boldsymbol{M} - \langle \boldsymbol{M} \rangle$, has off-diagonal entries with zero mean. The spectrum of $\mathcal{X}$ can be obtained via its average resolvent $\langle (z\boldsymbol{I} - \mathcal{X})^{-1} \rangle$, using the Stieltjes transform $\rho(z) = -(1/N\pi)\,\mathrm{Im}\,\mathrm{Tr}\langle (z\mathbf{I} - \mathcal{X})^{-1} \rangle$, with z approaching the real line from above. Given an arbitrary random matrix $\boldsymbol{X}$ with zero-mean off-diagonal entries, if the variance of the entries is sufficiently large, we can use the approximation [25]

$$\langle [\boldsymbol{X}^{-1}]_{ii} \rangle \simeq \sum_{X_{ii}} \frac{P^i(X_{ii})}{X_{ii} - \sum_j \langle [\boldsymbol{X}^{-1}]_{jj} \rangle \langle a_j^2 \rangle}, \tag{1}$$

and $\langle [\boldsymbol{X}^{-1}]_{ij} \rangle = 0$ for $i \neq j$, where $\boldsymbol{a}$ is the ith column of $\boldsymbol{X}$, with the diagonal element removed, and it is assumed that the diagonal elements X_{ii} can only take discrete values, distributed according to $P^i(X_{ii})$. We use Eq. (1) to compute the average resolvent of the matrix $\mathcal{X}$. We consider random graphs parametrized as stochastic block models [21–23] where N nodes are divided into B distinct blocks, where each block r has n_r nodes, and the matrix entry e_{rs} specifies the number of edges between blocks r and s, which are otherwise randomly placed. Hence, in the considered cases, the expected value of $\boldsymbol{M}$ is simply a function of the block memberships, i.e., $\langle C_{ii} \rangle = [\boldsymbol{C}_B]_{b_i,b_i} = c_{b_i}$ and $\langle M_{ij} \rangle = [\boldsymbol{M}_B]_{b_i,b_j}$, with $\boldsymbol{C}_B$ and $\boldsymbol{M}_B$ being matrices of size $B \times B$, and the vector $\boldsymbol{b}$ of size N and entries in the range $[1, B]$ specify the block memberships. When applying this to Eq. (1) with $\boldsymbol{X} = z\boldsymbol{I} - \mathcal{X}$, we may use the fact the averages on both sides of Eq. (1) can only depend on the block membership of the respective nodes. Thus, using the shorthand $t_r(z) \equiv \langle [(z\boldsymbol{I} - \mathcal{X})^{-1}]_{ii} \rangle$ for $i \in r$, we obtain

$$t_r(z) = \sum_c \frac{p_c^r}{z - c - \sum_s \sigma_{rs}^2 n_s t_s(z)}, \tag{2}$$

where p_c^r is the probability distribution of the diagonal elements c for block r, and σ_{rs}^2 is the variance of the elements of $\mathcal{M}$, labeled according to block membership, which is identical to the variance of $\boldsymbol{M}$. The spectrum of $\mathcal{X}$ may be finally obtained via

$$\rho(z) = -\frac{1}{N\pi} \sum_r n_r \mathrm{Im} t_r(z). \tag{3}$$

In order to obtain the spectrum of $\boldsymbol{W}$, we employ an argument developed in Ref. [26] and note that in order for z to be an eigenvalue of $\boldsymbol{W} = \mathcal{X} + \boldsymbol{M}$, we must have $\det[z\boldsymbol{I} - (\mathcal{X} + \langle \boldsymbol{M} \rangle)] = 0$, which can be rewritten as $\det(z\boldsymbol{I} - \mathcal{X}) \det[\boldsymbol{I} - (z\boldsymbol{I} - \mathcal{X})^{-1} \langle \boldsymbol{M} \rangle] = 0$. Thus, if the second determinant is zero for a given z, it will be an eigenvalue of $\boldsymbol{W}$ but not of $\mathcal{X}$. These additional eigenvalues may be obtained via the ensemble average $\det[\boldsymbol{I} - \langle (z\boldsymbol{I} - \mathcal{X})^{-1} \rangle \langle \boldsymbol{M} \rangle] = 0$, which will hold if the matrix $\langle (z\boldsymbol{I} - \mathcal{X})^{-1} \rangle \langle \boldsymbol{M} \rangle$ has an eigenvalue equal to one. Since this matrix has a maximum rank equal to B, its nonzero eigenvalues will be identical to the $B \times B$ matrix $\boldsymbol{T}(z)\boldsymbol{M}_B\boldsymbol{N}$, where $\boldsymbol{T}(z)$ and $\boldsymbol{N}$ are diagonal $B \times B$ matrices containing the values of $t_r(z)$ and n_r, respectively. Hence, the existence of additional eigenvalues of $\boldsymbol{W}$ may obtained by solving

$$\det[\boldsymbol{I}_B - \boldsymbol{T}(z)\boldsymbol{M}_B\boldsymbol{N}] = 0, \tag{4}$$

simultaneously with $\rho(z) = 0$. Equations (2)–(4) provide a complete recipe for obtaining the desired spectrum, provided we know the $B \times B$ matrices σ_{rs}^2 and $\boldsymbol{M}_B$ as well as the diagonal entry distribution p_c^r. For the three matrices of interest, they are easily computed as $\{p_c^r = \delta_{0,c}; \sigma_{rs}^2 = [\boldsymbol{M}_B]_{rs} = e_{rs}/n_r n_s\}$ for $\boldsymbol{A}$ and $\{p_c^r = P(c, e_r/n_r); [\boldsymbol{M}_B]_{rs} = -e_{rs}/n_r n_s; \sigma_{rs}^2 = e_{rs}/n_r n_s\}$ for $\boldsymbol{L}$, with $P(c, \lambda)$ being a Poisson distribution on c with average λ and $\{p_c^r = \delta_{1,c}; [\boldsymbol{M}_B]_{rs} = -e_{rs}/\sqrt{n_r e_r n_s e_s}; \sigma_{rs}^2 \simeq e_{rs}/e_r e_s\}$ for $\mathcal{L}$. We emphasize that, since the approximation in Eq. (1) was used, the obtained spectrum should be correct only in the limit of sufficiently large degrees. If this holds, the theory reproduces in very good detail the spectrum of empirical networks, as can be seen in Fig. 1. The spectrum is composed of a continuous band, as well as a number of isolated eigenvalues, which correspond very well to the solutions of Eqs. (3) and (4), respectively. The same is true for the spectrum of the matrices $\mathcal{L}$ and $\boldsymbol{L}$ (Fig. 2). The spectrum of $\boldsymbol{L}$ is special, since it contains an elaborate fine structure, with many fringes, and an interleaving of the continuous band [Eq. (3)] with the isolated eigenvalues

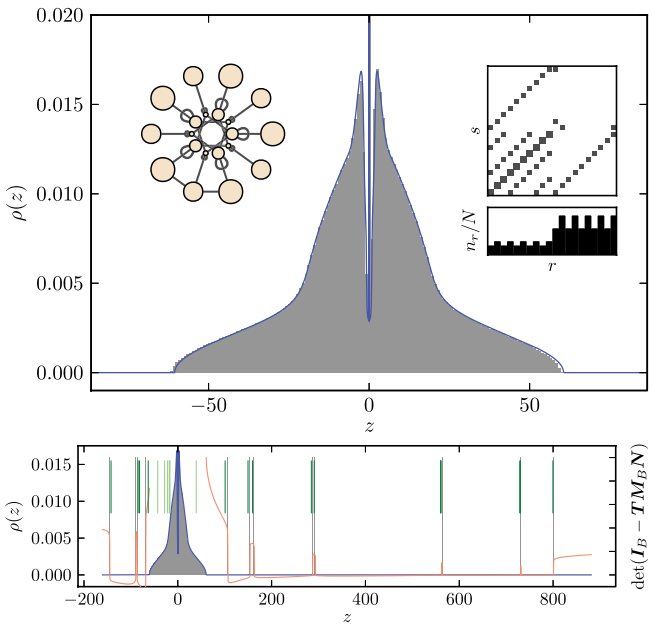

FIG. 1 (color online). Top: Continuous band of the matrix $\boldsymbol{A}$ for the block structure in the inset (right, e_{rs} matrix and block sizes n_r; left, graphical representation). The solid line corresponds to Eq. (3), and the gray histogram is averaged over 25 network realizations with $N = 2 \times 10^4$ and $\langle k \rangle = 300$. Bottom: The same, but with the isolated eigenvalues added. The gray vertical lines are average empirical values, whereas the solid (orange) curve corresponds to the determinant of Eq. (4). The vertical (green) line segments mark the eigenvalues of the matrix $\boldsymbol{C}_B + \boldsymbol{M}_B\boldsymbol{N}$.

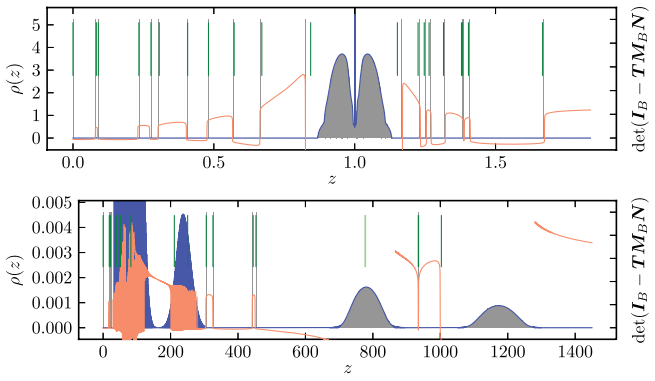

FIG. 2 (color online). Eigenvalue spectrum of the normalized Laplacian matrix $\mathcal{L}$ (top) and Laplacian matrix $\boldsymbol{L}$ (bottom) for the block structure of Fig. 1.

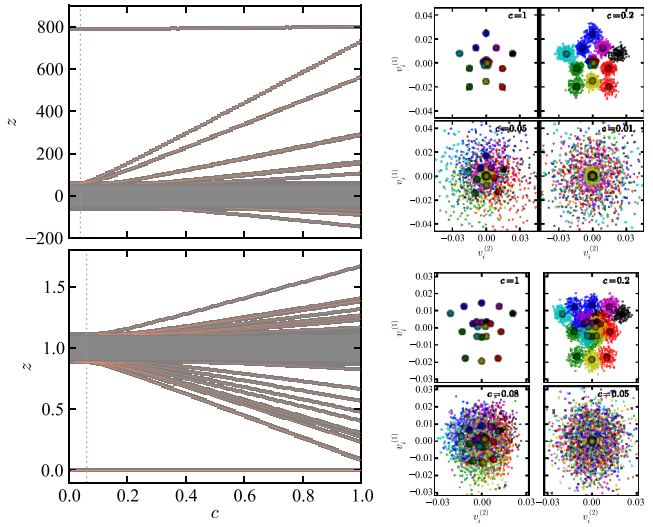

FIG. 3 (color online). Left: Extremal eigenvalues of $\boldsymbol{A}$ (top) and $\mathcal{L}$ (bottom), for the block structure of Fig. 1, as a function of the parameter c defined in the text. The solid lines are solutions of Eq. (4), and the data points are empirical values for $N = 2 \times 10^4$. The dotted vertical line marks the detachment transition. Right, top (bottom): Eigenvector values for the second and third largest (smallest) eigenvalues of $\boldsymbol{A}$ ($\mathcal{L}$), for different values of c. The circles (stars) correspond to the empirical (theoretical) average values for each block.

[Eq. (4)]. The continuous band has no well-defined edge, with fringes which extend through the whole spectrum, but with decaying amplitudes. Despite such a detailed structure, the theory captures these features very well, as can be seen in Fig. 2 (see also the Supplemental Material [27]).

For isolated eigenvalues which are sufficiently detached from the spectral band, Eq. (2) may be approximated by $t_r \approx 1/(z - c_r)$, in which case Eq. (4) amounts to $\det[z\boldsymbol{I}_B - (\boldsymbol{C}_B + \boldsymbol{M}_B\boldsymbol{N})] = 0$, where $\boldsymbol{C}_B$ is a diagonal matrix with the c_r values. If this holds, the detached eigenvalues will correspond to the spectrum of the matrix $\boldsymbol{C}_B + \boldsymbol{M}_B\boldsymbol{N}$.

At the edges of the continuous band, the purely real solution to Eq. (2) becomes unstable, and the largest eigenvalue of the Jacobian $J_{rs}(z) \equiv \partial \hat{t}_r/\partial t_s = \sum_c p_c^r \sigma_{rs}^2 n_s/[z - c - \sum_s \sigma_{rt}^2 n_t t_t(z)]^2$, where $\hat{t}_r$ is the right-hand side of Eq. (2), becomes equal to one. Hence, one may find the edges of the continuous band by solving $\det[\boldsymbol{I}_B - \boldsymbol{J}(z)] = 0$, simultaneously with $\rho(z) = 0$.

Eigenvectors.—The eigenvector equation $(\mathcal{X} + \boldsymbol{M})\boldsymbol{v} = z\boldsymbol{v}$ can be rewritten as $(z\boldsymbol{I} - \mathcal{X})^{-1}\boldsymbol{M}\boldsymbol{v} = \boldsymbol{v}$. Taking the ensemble average, we get $\langle (z\boldsymbol{I} - \mathcal{X})^{-1}\rangle \boldsymbol{M}\langle \boldsymbol{v}\rangle = \langle \boldsymbol{v}\rangle$. Since the average values of $\boldsymbol{v}$ can only depend on the block memberships and $\langle (z\boldsymbol{I} - \mathcal{X})^{-1}\rangle$ is diagonal, we get

$$\boldsymbol{T}(z)\boldsymbol{M}_B\boldsymbol{N}\boldsymbol{v}_B = \boldsymbol{v}_B, \tag{5}$$

where $\boldsymbol{v}_B$ contain the average values of $\boldsymbol{v}$ for each block.

If the block structure is made sufficiently tenuous, all but the most extremal detached eigenvalues will approach progressively the continuous band. At some point, before the graph becomes fully random, they will merge with the continuous band, and the associated eigenvectors will no longer convey any information on the existing block structure. An example is shown in Fig. 3, which shows the full spectrum of the block structure given by $e_{rs} = ce_{rs}^0 + (1 - c)e_r^0 e_s^0/2E$, with e_{rs}^0 being the same block structure shown in Fig. 1, and $e_r^0 = \sum_s e_{rs}^0$. The parameter c interpolates between a random graph ($c = 0$) and the original block structure ($c = 1$), while preserving the same degree distribution. As show in Fig. 3, for a specific value of $c = c^* > 0$, all but the most extremal eigenvalues merge with the continuous band, and for $c < c^*$, the eigenvector values are no longer discernibly correlated with the planted block structure. It is important to notice that the transition point c^* is different for the matrices $\boldsymbol{A}$ and $\mathcal{L}$, and thus the different spectra will have different sensitivities to the planted block structure. This can be seen in more detail by considering a simpler two-block system with $n_1/N = w$, $n_2/N = 1 - w$, and $e_{rs} = E[c\delta_{rs} + (1 - c)/2]$, which is a diagonal block structure with the parameter c controlling the block segregation and w the degree asymmetry [28]. In Fig. 4 is shown the extremal eigenvalues for the three matrices as a function of c, compared with empirical values. For the normalized Laplacian matrix $\mathcal{L}$, the extremal eigenvalue is very insensitive to the parameter w [29]. The matrix $\boldsymbol{A}$ displays, on the other hand, different transition points, depending on w, with larger values of c^* for larger degree asymmetries. The spectral band for the matrix $\boldsymbol{L}$ has no well-defined edge; hence, the transition point on a finite network will depend on the system size. The observable edge of the band is obtained by computing the extremal statistics of $\rho(z)$ (see the Supplemental Material [27]) and matches well the observed values, as can be seen in Fig. 4. A comparison of the transition points can be seen in the lower right of Fig. 4, where it is also included the values for the modularity matrix $\boldsymbol{B} = \boldsymbol{A} - \boldsymbol{k}\boldsymbol{k}^T/2E$, where $\boldsymbol{k}$ is a vector with node degrees, often used for

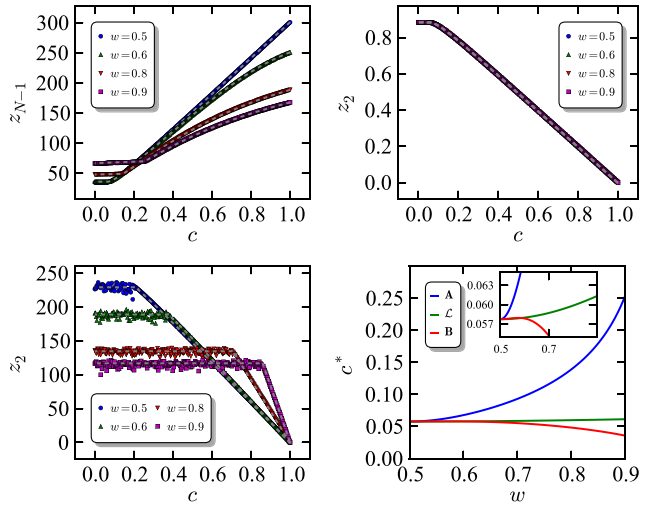

FIG. 4 (color online). Top, left (right): Second largest (smallest) eigenvalue of $\boldsymbol{A}$ ($\boldsymbol{\mathcal{L}}$), for the asymmetric two-block structure described in the text. The dashed curves are the theoretical values, and the data points are obtained from network realizations with $N = 2 \times 10^4$ and $\langle k \rangle = 300$. Bottom, left: Second smallest eigenvalue of L. The dashed curves are the expected values for $N = 2 \times 10^4$ (see the Supplemental Material [27]). Bottom, right: Transition point c^* as a function of w for the matrices $\boldsymbol{A}$ and $\boldsymbol{\mathcal{L}}$ and the modularity matrix $\boldsymbol{B}$.

community detection [18], which can also be calculated with the presented method in an entirely analogous fashion. Since for this specific block structure it has systematically the lowest threshold c^* among the others, this seems to corroborate the hypothesis in Refs. [16,30] that $\boldsymbol{B}$ may posses optimal characteristics in some scenarios. On the other hand, the comparatively worst behavior of the Laplacian $\boldsymbol{L}$ raises issues with its use for this purpose (as in, e.g., Ref. [31]).

Homogeneous blocks.—Further analytical progress can be made by assuming that the blocks are homogeneous, such that the right-hand side of Eq. (2) is the same for all blocks. This means that they must all share the same properties such as size n_r and average degree e_r/n_r. The solution in the case $p_c^r = \delta_{d,c_r}$ (i.e., for both $\boldsymbol{A}$ and $\boldsymbol{\mathcal{L}}$) will then be simply $t(z) = [z - d \pm \sqrt{(d-z)^2 - 4a}]/2a$ with $a = a_r = N\sum_s \sigma_{rs}^2/B$, which will result in the usual semicircle distribution $\rho(z) = \sqrt{4a - (z-d)^2}/2a\pi$ for $|z - d| < 2\sqrt{a}$; otherwise, $\rho(z) = 0$. The detached eigenvalues will be given by the solution of $\det[\boldsymbol{I} - t(z)N\boldsymbol{M}_B/B] = 0$. Hence, there will be a one-to-one correspondence between the nonzero eigenvalues λ_i of $\boldsymbol{M}_B$ and the detached eigenvalues $z_i = d + at_i + 1/t_i$, where $t_i = B/N\lambda_i$, as long as $|z_i - d| > 2\sqrt{a}$; otherwise, they will merge with the continuous band. By making $|z_i - d| = 2\sqrt{a}$, one obtains that this transition happens at $\lambda_i = \pm\sqrt{a}B/N$. Both for $\boldsymbol{A}$ and $\boldsymbol{\mathcal{L}}$, one can see that this transition occurs at the same point: If one writes the block matrix as $e_{rs} = N\langle k \rangle m_{rs}$, such that $\sum_{rs} m_{rs} = 1$, this transition translates to

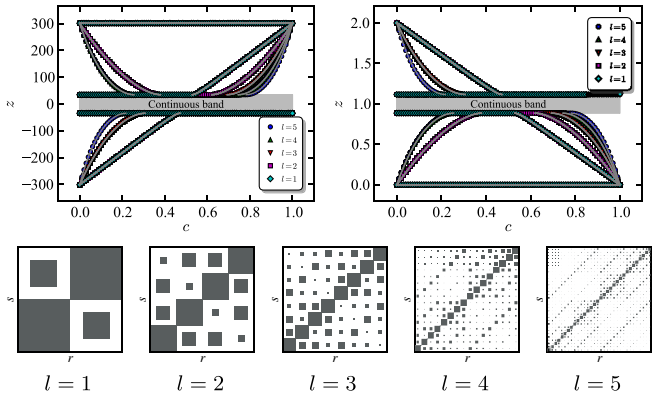

FIG. 5 (color online). Top: Detachment transitions for the nested partition model described in the text with $B_1 = 2$ as a function of the mixing parameter c, and for different nested depths l, for $\boldsymbol{A}$ and $\boldsymbol{\mathcal{L}}$. The data points correspond to network realizations with $N = 2 \times 10^4$ and $\langle k \rangle = 300$, and the solid lines are theoretical values. Bottom: Example of e_{rs} matrices with $B_1 = 2$ for different values of l.

$$\lambda_m^2 = \frac{1}{\langle k \rangle B^2}, \tag{6}$$

where λ_m is an eigenvalue of the m_{rs} matrix. The fact that the detachment transition is identical for both $\boldsymbol{A}$ and $\boldsymbol{\mathcal{L}}$ is a special property of the homogeneous block structure, and does not hold in general, as we have shown previously [32].

As a concrete example of an homogeneous structure, we consider a nested version of the usual planted partition model [33], inspired by similar constructions done in Refs. [34,35]. We define a seed structure with B_1 blocks and $[\boldsymbol{m}_1]_{rs} = \delta_{rs}c/B_1 + (1 - \delta_{rs})(1 - c)/B_1(B_1 - 1)$, and construct a nested matrix of depth l via $\boldsymbol{m}_l = \boldsymbol{m}_{l-1} \otimes \boldsymbol{m}_{l-1}$ where $\otimes$ denotes the Kronecker product. The eigenvalues of the matrix $\boldsymbol{m}_l$ are given by $\lambda_{m_l}^i = \{(cB_1 - 1)/[B_1(B_1 - 1)]\}^{l-i}/B_1^i$, for $i \in [0, l]$. Thus, from Eq. (6), one obtains a series of transitions, where a deeper level of the nested structure "fades away," and the spectrum is indistinguishable from that of a $l - 1$ structure (see Fig. 5). The transition of the shallowest level happens at $\langle k \rangle = [(B - 1)/(cB - 1)]^2$, which is the same as the regular planted partition model [16]. This transition marks the point at which more general inference methods should also fail to detect the imposed partition [36].

In summary, we presented an unified framework to obtain the full spectrum of random networks with modular structure, in the limit of large degrees. We showed that the detachment transition of the isolated eigenvalues is a general feature which determines how strongly the existing modular structure affects the different spectra. The different matrices react differently to the imposed modular structure and have different transition points. Only when the blocks are homogeneous do some of these transitions collapse together. Hence, in general, the detectability threshold of the imposed block structure may depend strongly on the actual spectrum which is observed.

*tiago@itp.uni-bremen.de

[1] J. D. Noh and H. Rieger, Phys. Rev. Lett. **92**, 118701 (2004).
[2] A. N. Samukhin, S. N. Dorogovtsev, and J. F. F. Mendes, Phys. Rev. E **77**, 036115 (2008).
[3] M. Barahona and L. M. Pecora, Phys. Rev. Lett. **89**, 054101 (2002).
[4] A. Arenas, A. Díaz-Guilera, J. Kurths, Y. Moreno, and C. Zhou, Phys. Rep. **469**, 93 (2008).
[5] J. A. Almendral and A. Díaz-Guilera, New J. Phys. **9**, 187 (2007).
[6] Y. Wang, D. Chakrabarti, C. Wang, and C. Faloutsos, in *Proceedings of the 22nd International Symposium on Reliable Distributed Systems, 2003* (IEEE, New York, 2003), pp. 25–34.
[7] C. Castellano and R. Pastor-Satorras, Phys. Rev. Lett. **105**, 218701 (2010).
[8] A. V. Goltsev, S. N. Dorogovtsev, J. G. Oliveira, and J. F. F. Mendes, Phys. Rev. Lett. **109**, 128702 (2012).
[9] S. N. Dorogovtsev, A. V. Goltsev, J. F. F. Mendes, and A. N. Samukhin, Phys. Rev. E **68**, 046109 (2003).
[10] F. Chung, L. Lu, and V. Vu, Proc. Natl. Acad. Sci. U.S.A. **100**, 6313 (2003).
[11] D.-H. Kim and A. E. Motter, Phys. Rev. Lett. **98**, 248701 (2007).
[12] M. E. J. Newman, Nat. Phys. **8**, 25 (2011).
[13] G. Ergün and R. Kühn, J. Phys. A **42**, 395001 (2009).
[14] R. Kühn and J. van Mourik, J. Phys. A **44**, 165205 (2011).
[15] S. Chauhan, M. Girvan, and E. Ott, Phys. Rev. E **80**, 056114 (2009).
[16] R. R. Nadakuditi and M. E. J. Newman, Phys. Rev. Lett. **108**, 188701 (2012).
[17] S. Fortunato, Phys. Rep. **486**, 75 (2010).
[18] M. E. J. Newman, Phys. Rev. E **74**, 036104 (2006).
[19] M. Fiedler, Czech. Math. J. **23**, 298 (1973).
[20] A. Pothen, H. D. Simon, and K.-P. Liou, SIAM J. Matrix Anal. Appl. **11**, 430 (1990).
[21] P. W. Holland, K. B. Laskey, and S. Leinhardt, Soc. Networks **5**, 109 (1983).
[22] S. E. Fienberg, M. M. Meyer, and S. S. Wasserman, J. Am. Stat. Assoc. **80**, 51 (1985).
[23] K. Faust and S. Wasserman, Soc. Networks **14**, 5 (1992).
[24] B. Karrer and M. E. J. Newman, Phys. Rev. E **83**, 016107 (2011).
[25] R. R. Nadakuditi and M. E. J. Newman, Phys. Rev. E **87**, 012803 (2013).
[26] F. Benaych-Georges and R. R. Nadakuditi, Adv. Math. **227**, 494 (2011).
[27] See Supplemental Material at http://link.aps.org/supplemental/10.1103/PhysRevLett.111.098701 for more information on the system size dependence of the measurable spectrum of the Laplacian matrix $\boldsymbol{L}$.
[28] Note that the parameter c does not change the degree distribution.
[29] The curves *do* change, however, only very subtly.
[30] F. Radicchi, Phys. Rev. E **88**, 010801(R) (2013).
[31] M. E. J. Newman, Europhys. Lett. **103** 28 003 (2013).
[32] It can also be shown that Eq. (6) also holds for the modularity matrix $\boldsymbol{B}$.
[33] A. Condon and R. M. Karp, Random Struct. Algorithms **18**, 116 (2001).
[34] J. Leskovec, D. Chakrabarti, J. Kleinberg, C. Faloutsos, and Z. Ghahramani, arXiv:0812.4905.
[35] G. Palla, L. Lovász, and T. Vicsek, Proc. Natl. Acad. Sci. U.S.A. **107**, 7640 (2010).
[36] A. Decelle, F. Krzakala, C. Moore, and L. Zdeborová, Phys. Rev. Lett. **107**, 065701 (2011).